

Continuum Theory of Edge States of Topological Insulators: Variational Principle and Boundary Conditions

Amal Medhi* and Vijay B. Shenoy†

Center for Condensed Matter Theory, Indian Institute of Science, Bangalore 560012, India

(Dated: October 22, 2018)

We develop a continuum theory to model low energy excitations of a generic four-band time reversal invariant electronic system with boundaries. We propose a variational energy functional for the wavefunctions which allows us derive natural boundary conditions valid for such systems. Our formulation is particularly suited to develop a continuum theory of the protected edge/surface excitations of topological insulators both in two and three dimensions. By a detailed comparison of our analytical formulation with tight binding calculations of ribbons of topological insulators modeled by the Bernevig-Hughes-Zhang (BHZ) hamiltonian, we show that the continuum theory with the natural boundary condition provides an appropriate description of the low energy physics. As a spin-off, we find that in a certain parameter regime, the gap that arises in topological insulator ribbons of finite width due to the hybridization of edges states from opposite edges, depends non-monotonically on the ribbon width and can nearly vanish at certain “magic widths”.

PACS numbers: 73.20.At, 73.21.Fg, 73.43.-f

I. INTRODUCTION

One of the physically observable phenomena in topological insulators (TI) is the existence of the linearly dispersing gapless edge (in two dimension (2D) or surface (in three dimension (3D)) states which are topologically protected against moderate electronic interactions or nonmagnetic disorder.¹⁻⁵ The fact that these conducting edge states can host spin current without dissipation makes topological insulators (TI) a promising candidate in technological applications.^{6,7} Understanding the nature of the edge states has been an aspect of interest in theoretical studies of topological insulators.⁸⁻¹²

Properties of edge states can be studied by constructing appropriate tight binding model Hamiltonians of TIs and examining their eigenstates for lattices with boundaries. An alternative route is to construct a low energy continuum theory^{3,9,13} that allows for analytical treatment that aids the development of field theoretic description in the presence of interactions.^{14,15} Such approaches have been gainfully employed earlier in studies of graphene.¹⁶⁻²⁰ In the analytic calculation, the edge states are obtained by subjecting appropriate boundary condition (BC) on the wavefunction. Here one usually⁸⁻¹² imposes the *fixed* boundary condition (also called as *essential* or Dirichlet boundary condition in the mathematical literature²¹) where the wavefunction is assumed to be zero at the boundaries or at a fictitious layer of atoms just outside the boundaries. Such a choice of BC constrains the nature of the wavefunction in that the maximum weight of the edge state does not occur in the edge layers but in bulk layers that are near the edge layer. In the presence of interactions, the edge states and bulk states mix and the ensuing physics is determined crucially by this mixing. In a recent study²², it was shown that the Mott transition in topological insulator ribbons can occur in two different routes – the synchronous and asynchronous routes – depending on the nature of edge

states. A continuum field theoretic analysis of such a phenomenon, therefore, requires a careful treatment of the edge states so that their profile correctly captures the mixing with the bulk states.

With this motivation, in this paper, we develop a continuum theory of time reversal invariant four-band model Hamiltonians that have been extensively used in the analysis of topological insulators in two and three dimensions. We construct an energy functional of the wave functions; the wave function that renders this energy functional extremum is shown to satisfy a stationary Schrödinger equation that matches the four-band lattice theory at long wavelengths. As a key outcome of this approach, we derive a new boundary condition, the *natural* boundary condition.²¹ This boundary condition is valid for any four-band time reversal invariant system in two and three dimensions. We use the BHZ model³ that has been studied earlier⁸⁻¹¹ to show that within a regime of parameters of this model, the natural boundary condition provides an excellent description of the edge states. In the process of this study, we show that the gap that arises from the hybridization of the edge states localized on the opposite edges of a ribbon is a non-monotonic function of the ribbon width. This finding could potentially be useful in many applications such as design of thermoelectric devices etc.^{23,24}

In the following section (sec. II) we introduce a general four-band lattice Hamiltonian that is time reversal invariant. Sec. III contains the continuum theory of these systems, the formulation of a variational principle and derivation of the boundary conditions. A detailed comparison of the numerical tight binding calculations and the analytical continuum theory is carried out in sec. IV using the BHZ model,³ in its topological regime. The paper is concluded in sec. V which contains a discussion, significance and summary of the results.

II. FOUR-BAND TIME REVERSAL INVARIANT SYSTEMS

Consider a Bravais lattice in two or three dimensions whose sites are labelled by I . Each lattice site has two orbitals (or “basis” sites such as A-B sites in the graphene lattice, sometimes also referred to as “flavours”) labelled by α . The operator $C_{I\alpha\sigma}^\dagger$ creates an electron of spin σ (quantized along some convenient axis) in the orbital α at site I . The Hamiltonian of the system is given by

$$\mathcal{H} = - \sum_{I\delta} t_{\alpha\sigma,\beta\sigma'}(\delta) C_{(I+\delta)\alpha\sigma}^\dagger C_{I\beta\sigma'} \quad (1)$$

where δ runs over lattice vectors, summation over repeated orbital and spin indices is implied. The hopping matrix elements $t_{\alpha\sigma,\beta\sigma'}(\delta)$ are such that the Hamiltonian eqn. (1) is time reversal invariant. Hamiltonians discussed in the literature on topological insulators^{4,5} are of this type.

With the aim of developing a long wavelength continuum theory of such systems, we cast the Hamiltonian in the reciprocal space:

$$\mathcal{H} = \sum_{\mathbf{k} \in \mathcal{B}} H_{ab}(\mathbf{k}) C_{\mathbf{k}a}^\dagger C_{\mathbf{k}b} \quad (2)$$

where a (and b) is an index that represents the composite $\alpha\sigma$. Repeated a and b indices are summed over and \mathbf{k} runs over \mathcal{B} , the Brillouin zone which is a torus for 2D systems and a 3-torus in 3D systems. Following Refs. [1, 25, and 26], we now write the matrix $H(\mathbf{k})$ in a basis of sixteen 4×4 matrices, broken up into two groups Γ^m ($m = 0 - 5$) and Λ^n ($n = 1 - 10$), i.e.,

$$H(\mathbf{k}) = \sum_{n=0}^5 d_n(\mathbf{k}) \Gamma^n + \sum_{m=1}^{10} e_m(\mathbf{k}) \Lambda^m \quad (3)$$

where $d_n(\mathbf{k})$ and $e_m(\mathbf{k})$ are smooth functions of \mathbf{k} . The matrices Γ and Λ are defined using $\boldsymbol{\tau}$ and $\boldsymbol{\sigma}$, the 2×2 Pauli matrices associated with the orbital and spin degrees of freedom, and $\mathbf{1}$, the 2×2 identity matrix. We have, $\Gamma^0 = \mathbf{1} \otimes \mathbf{1}$,

$$\Gamma^{1,2,3,4,5} = \{ \boldsymbol{\tau}^x \otimes \mathbf{1}, \boldsymbol{\tau}^z \otimes \mathbf{1}, \boldsymbol{\tau}^y \otimes \boldsymbol{\sigma}^x, \boldsymbol{\tau}^y \otimes \boldsymbol{\sigma}^y, \boldsymbol{\tau}^y \otimes \boldsymbol{\sigma}^z \} \quad (4)$$

The ten elements Λ^m , $m = 1, \dots, 10$ can be obtained from the commutators $[\Gamma^n, \Gamma^{n'}]/(2i)$, $n = 1, \dots, 5, n' > n$. The grouping of these matrices into Γ s and Λ s is motivated by the fact that under the action of the time reversal operator $\Theta = -i(\mathbf{1} \otimes \boldsymbol{\sigma}^y)K$ where K is the complex conjugation operator²⁷, $\Theta^{-1}\Gamma^n\Theta = \Gamma^n$ while $\Theta^{-1}\Lambda^m\Theta = -\Lambda^m$. From the fact that the Hamiltonian in eqn. (2) is time reversal invariant, and from the properties of the Γ and Λ matrices just mentioned, we get from eqn. (3) that¹

$$\begin{aligned} d_n(-\mathbf{k}) &= d_n(\mathbf{k}) \\ e_m(-\mathbf{k}) &= -e_m(\mathbf{k}) \end{aligned} \quad (5)$$

Eqn. 2 along with eqns. 3 and 5 describes a general four-band Hamiltonian with time reversal symmetry.

The systems of interest are those which possess a gap in their energy dispersion – two bands and separated from the other two by an energy gap – and the chemical potential lies in this gap. The nature of this insulating state (topological or trivial) is determined by the topological properties of the occupied bands and is characterized by the Z_2 index.^{1-3,28-30} While our formulation is applicable to any four-band system with time reversal symmetry, we shall focus on topological insulators which possess protected edge/surface states.

III. CONTINUUM THEORY, VARIATIONAL PRINCIPLE AND BOUNDARY CONDITIONS

The continuum theory is developed by focusing on a region of the Brillouin zone, i. e., specifically around the \mathbf{k} -points which support low energy excitations. In the case of topological insulators with a bounding edge (or surface), the low energy excitations (i. e., excitations close to the chemical potential) usually occur near a time reversal invariant momentum (TRIM).⁴ TRIMs occur at the origin of the Brillouin zone, at the zone edges etc. In what follows, we shall develop the continuum theory focusing on the $\mathbf{k} = \mathbf{0}$ TRIM; generalization to any other TRIM of interest is straightforward.

We discuss the continuum theory in the first quantized form. For our four-band model, the wave function is a four component vector function $\psi_a(\mathbf{x})$ of the position \mathbf{x} . We look to determine a Hamiltonian operator \mathbb{H} that dictates the time evolution of $\psi_a(\mathbf{x})$, i. e.,

$$i\dot{\psi}_a(\mathbf{x}) = \mathbb{H}_{ab}\psi_b(\mathbf{x}) \quad (6)$$

where the dot represents time derivative and the repeated index b is summed over. We have set $\hbar = 1$. To determine \mathbb{H} , we expand the function $d_n(\mathbf{k})$ and $e_m(\mathbf{k})$ about $\mathbf{k} = \mathbf{0}$ up to quadratic order, which upon using eqn. (5) gives

$$\begin{aligned} d_n(\mathbf{k}) &= d_n^0 + k_i S_{ij}^n k_j \\ e_m(\mathbf{k}) &= 2A_i^m k_i \end{aligned} \quad (7)$$

where the constants d_n^0 , tensors S_{ij}^n and vectors A_i^n are properties of the four-band system that characterize the dispersion near $\mathbf{k} = \mathbf{0}$. We thus have

$$H_{ab}(\mathbf{k}) \approx (d_n^0 + S_{ij}^n k_i k_j) \Gamma_{ab}^n + 2A_i^m k_i \Lambda_{ab}^m \quad (8)$$

where repeated n and m indices are summed over the ranges indicated in eqn. (3). \mathbb{H}_{ab} can now be obtained as $\mathbb{H}_{ab} = H_{ab}(k_i \rightarrow -i\partial_i)$ where $\partial_i \equiv \partial/\partial x_i$, i. e.,

$$\mathbb{H}_{ab} = (d_n^0 - S_{ij}^n \partial_i \partial_j) \Gamma_{ab}^n - 2iA_i^m \partial_i \Lambda_{ab}^m \quad (9)$$

which completes the discussion of eqn. (6).

Consider now a region of space (in two or three dimensions) Ω bounded by a boundary $\partial\Omega$ (which may be an

edge or a surface). The stationary states at low energy are eigenstates of the continuum Hamiltonian \mathbb{H} , i. e.,

$$\mathbb{H}_{ab}\Psi_b(\mathbf{x}) = E\Psi_a(\mathbf{x}) \quad (10)$$

where E is the energy eigenvalue, with appropriate boundary conditions for the four component wavefunction $\Psi_a(\mathbf{x})$ on $\partial\Omega$.

To aid the determination of the boundary conditions, here we propose an energy functional associated with a four component wavefunction $\Psi_a(\mathbf{x})$:

$$\mathcal{E}[\Psi^*(\mathbf{r}), \Psi(\mathbf{r})] = \int_{\Omega} d^d\mathbf{r} \left(\Psi_a^* d_n^0 \Gamma_{ab}^n \Psi_b - (\partial_i \Psi_a^*) S_{ij}^n \Gamma_{ab}^n (\partial_j \Psi_b) - i [\Psi_a^* A_i^m \Lambda_{ab}^m \partial_i \Psi_b + (\partial_i \Psi_a^*) A_i^m \Lambda_{ab}^m \Psi_b] - E \Psi_a^* \Psi_a \right) \quad (11)$$

where E is a Lagrange multiplier that ensures that the wavefunction is normalized to unity. All repeated indices are summed over their appropriate ranges. We now show that the states that render this energy functional extremal are the stationary states of eqn. (10). Towards this end, upon varying Ψ^* by $\delta\Psi^*$, we get

$$\begin{aligned} \delta\mathcal{E} &= \int_{\Omega} d^d\mathbf{r} \left((\delta\Psi_a^*) d_n^0 \Gamma_{ab}^n \Psi_b - (\partial_i (\delta\Psi_a^*)) S_{ij}^n \Gamma_{ab}^n (\partial_j \Psi_b) - i [(\delta\Psi_a^*) A_i^m \Lambda_{ab}^m \partial_i \Psi_b + (\partial_i (\delta\Psi_a^*)) A_i^m \Lambda_{ab}^m \Psi_b] - E (\delta\Psi_a^*) \Psi_a \right) \\ &= \int_{\Omega} d^d\mathbf{r} (\delta\Psi_a^*) \left[((d_n^0 - S_{ij}^n \partial_i \partial_j) \Gamma_{ab}^n - 2i A_i^m \partial_i \Lambda_{ab}^m - E \delta_{ab}) \Psi_b \right] + \int_{\partial\Omega} d^{d-1}\mathbf{r} (\delta\Psi_a^*) \left[n_i (S_{ij}^n \Gamma_{ab}^n \partial_j \Psi_b + i A_i^m \Lambda_{ab}^m \Psi_b) \right] \end{aligned} \quad (12)$$

where we have used the divergence theorem and n_i is the outward normal to the boundary $\partial\Omega$.

The extremality of \mathcal{E} necessitates that

$$((d_n^0 - S_{ij}^n \partial_i \partial_j) \Gamma_{ab}^n - 2i A_i^m \partial_i \Lambda_{ab}^m - E \delta_{ab}) \Psi_b = 0 \quad (13)$$

in Ω which is exactly the stationary Schrödinger equation of eqn. (10). Further on the boundary $\partial\Omega$, we have either

$$\delta\Psi_a^* = 0 \quad (14)$$

which corresponds the *fixed* boundary condition where the values of the wavefunction Ψ_a is fixed (usually to zero), or

$$n_i (S_{ij}^n \Gamma_{ab}^n \partial_j \Psi_b + i A_i^m \Lambda_{ab}^m \Psi_b) = 0 \quad (15)$$

which is the *natural* boundary condition (note, again, that all the repeated indices are summed). We emphasize that this boundary condition is applicable to any time reversal invariant four-band system in two or three dimensions. In particular, the formulation is tailor made for the study of edge (surface) states of topological insulators. In the next section, we illustrate this framework by calculating (analytically) the edge states of a topological insulator described by the well known BHZ model³.

IV. BHZ MODEL: COMPARISON OF CONTINUUM THEORY AND TIGHT BINDING RESULTS

The BHZ model³ describes 2D topological insulators realized in the HgTe/CdTe quantum wells. The tight binding version of the model is obtained by considering four spin-orbit coupled orbitals- $|s \uparrow\rangle$, $|p \uparrow\rangle \equiv |(p_y + ip_x) \uparrow\rangle$, $|s \downarrow\rangle$, and $|p \downarrow\rangle \equiv |(p_y - ip_x) \downarrow\rangle$ per site

on a square lattice whose lattice spacing a is taken as unity. The model can be written as,

$$\mathcal{H} = \sum_{I\alpha\sigma} \epsilon_{\alpha} C_{I\alpha\sigma}^{\dagger} C_{I\alpha\sigma} - \sum_{I\delta\alpha\beta\sigma} t_{\alpha\beta}(\delta\sigma) C_{(I+\delta)\alpha\sigma}^{\dagger} C_{I\beta\sigma} \quad (16)$$

where $\alpha, \beta = s, p$ and ϵ_{α} denote the orbital energies. $\sigma = \uparrow, \downarrow$ and δ is a nearest neighbour vector. The hopping matrix elements $t_{\alpha\beta}(\delta\sigma)$ in the $|s\sigma\rangle$, $|p\sigma\rangle$ basis are given by,

$$t(\pm\hat{x}\sigma) = \begin{pmatrix} t_{ss} & \pm\sigma \frac{it_{sp}}{\sqrt{2}} \\ \pm\sigma \frac{it_{sp}}{\sqrt{2}} & -t_{pp} \end{pmatrix}, \quad t(\pm\hat{y}\sigma) = \begin{pmatrix} t_{ss} & \pm \frac{t_{sp}}{\sqrt{2}} \\ \mp \frac{t_{sp}}{\sqrt{2}} & -t_{pp} \end{pmatrix} \quad (17)$$

where t_{ss} , t_{sp} , t_{pp} are overlap integrals and $\sigma = +1$ (-1) for spin \uparrow (\downarrow). In the reciprocal space, as in eqn. (2), this Hamiltonian is described by matrices

$$H(\mathbf{k}) = \begin{pmatrix} h(\mathbf{k}) & 0 \\ 0 & h^*(-\mathbf{k}) \end{pmatrix} \quad (18)$$

where

$$h(\mathbf{k}) = \begin{pmatrix} \epsilon_s - 2t_s (\cos k_x + \cos k_y) & 2t_{sp} (\sin k_x - i \sin k_y) \\ 2t_{sp} (\sin k_x + i \sin k_y) & \epsilon_p + 2t_s (\cos k_x + \cos k_y) \end{pmatrix} \quad (19)$$

where we have set $t_{ss} = t_{pp} = t_s$. Further defining ϵ_0 such that $\epsilon_s = -(\epsilon_0 - 4t_s)$ and $\epsilon_p = (\epsilon_0 - 4t_s)$ we have

$$H(\mathbf{k}) = d_2(\mathbf{k})\Gamma^2 + e_1(\mathbf{k})\Lambda^1 + e_2(\mathbf{k})\Lambda^2 \quad (20)$$

in the form of eqn. (3), with $\Gamma^2 = \tau^z \otimes \mathbb{1}$, $\Lambda^1 = \tau^x \otimes \sigma^z$, $\Lambda^2 = \tau^y \otimes \mathbb{1}$ and

$$\begin{aligned} d_2(\mathbf{k}) &= -\epsilon_0 + 2t_s(2 - (\cos k_x + \cos k_y)) \\ e_1(\mathbf{k}) &= 2t_{sp} \sin k_x \\ e_2(\mathbf{k}) &= 2t_{sp} \sin k_y \end{aligned} \quad (21)$$

All other $d(\mathbf{k})$ -s and $e(\mathbf{k})$ -s are zero. Note that here we have relabelled the m index in eqn. (3) for convenience. With this, focusing on the TRIM at $\mathbf{k} = \mathbf{0}$, we get the continuum Hamiltonian operator as

$$\mathbb{H} = (-\epsilon_0 - t_s(\partial_x^2 + \partial_y^2)) \Gamma^2 - 2it_{sp}\partial_x\Lambda^1 - 2it_{sp}\partial_y\Lambda^2 \quad (22)$$

with $d_2^0 = -\epsilon_0$, $S_{ij}^2 = t_s\delta_{ij}$, $A_x^1 = t_{sp}$, $A_y^2 = t_{sp}$; all other d -s, S -s, A -s are zero. This Hamiltonian, upon setting $t_s = 1$ has two scales, ϵ_0 and t_{sp} . When $\epsilon_0 > 0$, the system is in the topological phase; the remainder of the discussion considers only this case. The quantity t_{sp} is a measure of the hybridization of the s and p orbitals and determines the ‘‘multi-componentness’’ of the wavefunctions. It must be noted that this model conserves the spin quantum number, i. e., the \uparrow and \downarrow spins decouple at the one particle level.

In order to study the edge states of this model, we consider a geometry with $\Omega = (-\infty, \infty) \times (0, L)$, i. e., and infinitely long (along x -direction) ribbon of width L (terminated at $y = 0$ and $y = L$, i. e. $\partial\Omega = (y = 0) \cup (y = L)$). When $L \rightarrow \infty$, we get a half-space.

Since the spins sectors decouple, we shall consider only the \uparrow -spin sector; the results of the \downarrow -spin sector can be obtained by a time reversal operation. Exploiting the translational invariance along the x -direction, we write $\Psi_\alpha(x, y) = e^{ikx}\Psi_\alpha(y)$. For a given momentum k , the functions $\Psi_\alpha(y)$ satisfy eqn. (10) with \mathbb{H} given by eqn. (22):

$$\begin{pmatrix} -\epsilon_0 + t_s(k^2 - \partial_y^2) & 2t_{sp}(k - \partial_y) \\ 2t_{sp}(k + \partial_y) & \epsilon_0 - t_s(k^2 - \partial_y^2) \end{pmatrix} \begin{pmatrix} \Psi_s \\ \Psi_p \end{pmatrix} = E \begin{pmatrix} \Psi_s \\ \Psi_p \end{pmatrix} \quad (23)$$

Defining $\Phi = \Psi_s + \Psi_p$, $\Psi = \Psi_s - \Psi_p$, $G(D) \equiv G(\partial_y) = -\epsilon_0 + t_s(k^2 - \partial_y^2)$ and $H(D) \equiv H(\partial_y) = -2t_{sp}\partial_y$, we get

$$\begin{aligned} G(D)\Psi - H(D)\Psi &= (E - 2t_{sp}k)\Phi \\ G(D)\Phi + H(D)\Phi &= (E + 2t_{sp}k)\Psi \end{aligned} \quad (24)$$

which leads to

$$[G(D) - H(D)][G(D) + H(D)]\Phi = (E^2 - 4t_{sp}^2k^2)\Phi \quad (25)$$

Assuming a trial solution $\Phi(y) = e^{qy}$, we obtain the following quartic equation for q ,

$$t_s^2(k^2 - q^2)^2 + 2(-\epsilon_0t_s + 2t_{sp}^2)(k^2 - q^2) + (\epsilon_0^2 - E^2) = 0 \quad (26)$$

which gives four solutions for q , $q_{1,2} = \pm q_I$, $q_{3,4} = \pm q_{II}$ which are given by,

$$q_{I,II}^2 = k^2 + \frac{(-\epsilon_0t_s + 2t_{sp}^2) \pm \sqrt{4t_{sp}^2(t_{sp}^2 - \epsilon_0t_s) + t_s^2E^2}}{t_s^2} \quad (27)$$

Therefore the general solution for Φ and Ψ are given by,

$$\Phi(y) = \mathcal{A}_1e^{q_1y} + \mathcal{A}_2e^{q_2y} + \mathcal{A}_3e^{q_3y} + \mathcal{A}_4e^{q_4y} \quad (28)$$

$$\Psi(y) = \frac{1}{E + 2t_{sp}k} \{G(D) + H(D)\} \Phi(y) \quad (29)$$

where \mathcal{A}_i -s are four constants. The complete solution for the wavefunction is given by,

$$\Psi_\alpha(x, y) \equiv \begin{pmatrix} \Psi_s \\ \Psi_p \end{pmatrix} e^{ikx} = \frac{1}{2} \begin{pmatrix} \Phi + \Psi \\ \Phi - \Psi \end{pmatrix} e^{ikx} \quad (30)$$

The determination of the energy eigenvalue E and the constants \mathcal{A}_i -s requires the boundary conditions. The fixed boundary condition⁹ eqn. (14) reads

$$\begin{aligned} \Psi_s(0) = \Psi_p(0) &= 0 \\ \Psi_s(L) = \Psi_p(L) &= 0 \end{aligned} \quad (31)$$

while the natural boundary condition derived in eqn. (15) provides

$$\begin{aligned} t_s \frac{d\Psi_s}{dy} + t_{sp}\Psi_p &= 0 \\ t_s \frac{d\Psi_p}{dy} + t_{sp}\Psi_s &= 0 \end{aligned} \quad (32)$$

on $\partial\Omega$ i.e., at $y = 0$ and $y = L$.

In the remainder of the discussion t_s is set to unity. It is useful to discuss the nature of the solution of q , before proceeding to compare the analytical results with the numerical tight binding calculations. Note that the values of q depends on the energy eigenvalue E (eqn. (27)). Since the $\mathbf{k} = \mathbf{0}$ corresponds to a TRIM, we expect pair (time reversal related) of topologically protected edge states at $k = 0$, and by the symmetry of the problem, we expect $E = 0$ to be their energy eigenvalue. The values of q with $E = 0$ are then determined by the parameters ϵ_0 and t_{sp} , i. e., they are characterized by the same parameters that determine the ‘‘topology’’ of the system. Fig. 1 shows a plot of the qs as a function of the parameter ϵ_0 . We find that there are two regimes of ϵ_0 , $\epsilon_0 < t_{sp}^2$, where there are four distinct real roots for qs and $\epsilon_0 > t_{sp}^2$ where qs are complex and appear in conjugate pairs. In the former regime, magnitudes of q_1 and q_2 increase with increasing ϵ_0 , while that of q_3 and q_4 decrease with increasing ϵ_0 . In the latter regime, the real parts of q are unaffected, while their imaginary parts increase in magnitude. Clearly, the nature of the edge states for $\epsilon_0 < t_{sp}^2$ is different from that for $\epsilon_0 > t_{sp}^2$. In the former case, the edge state wavefunction is non-oscillating and falls exponentially as the distance from the edge. In the latter case, the wave function also has an oscillatory part, and as we shall show later, this leads to quite interesting physics and possibilities.

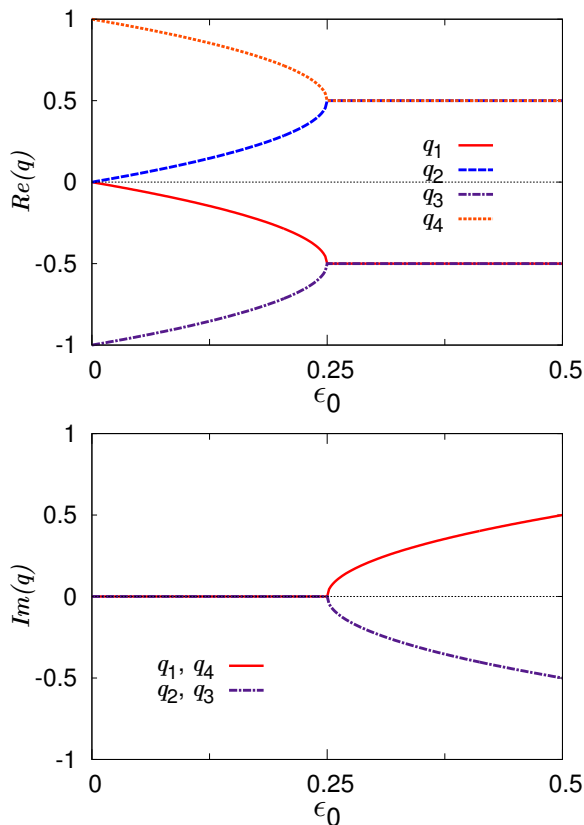


FIG. 1. The dependence of the wavevectors q that determine the nature of the edge states on ϵ_0 . Top: Real part of q . Bottom: Imaginary part of q . For $\epsilon_0 < t_{sp}^2$, the edge states are exponentially decaying, while for $\epsilon_0 > t_{sp}^2$, they have an oscillating character along with the exponential decay.

A. Half Space

Let us first consider a semi-infinite plane with its boundary at $y = 0$. Then the bounded solution for ϕ is given by,

$$\phi(y) = \mathcal{A}_2 e^{-q_1 y} + \mathcal{A}_4 e^{-q_1 i y} \quad (33)$$

The energy eigenvalues and the wave functions can be determined by imposing either the fixed boundary condition eqn. (31) or the natural boundary condition eqn. (32). After some simple algebra, it can be shown that for small k ,

$$E(k) = 2t_{sp}k \quad (34)$$

a linear dispersion for the edge states, that is, remarkably, *independent* of which boundary condition is chosen.

This value of $E(k)$ can be now used to determine the constant coefficients $\mathcal{A}_{2,4}$ and hence $\Psi_{s,p}$. The profile of the wave function, of course, depends strongly on the boundary conditions. Fig. 2 shows a comparison of the results of the analytical formulation presented above with the two different boundary conditions and the wave function obtained from numerical calculations with the full

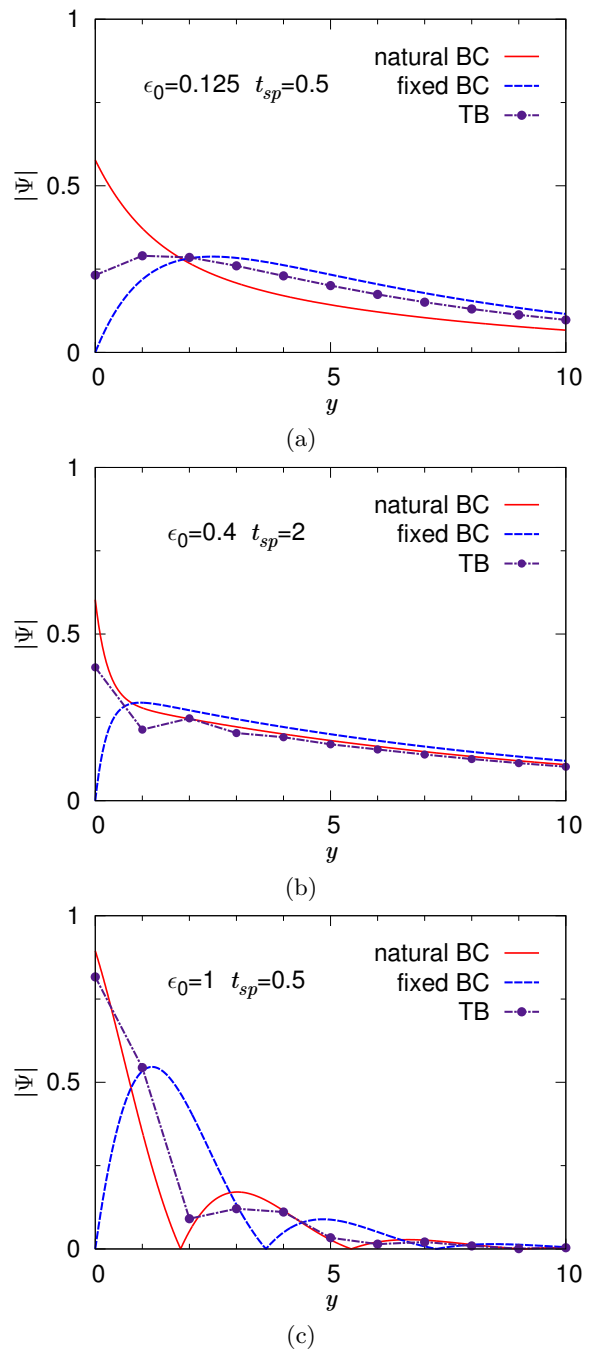


FIG. 2. Comparison of the edge state wavefunctions obtained analytically by using the two different BCs with the corresponding result from the tight binding calculation. The wavefunctions plotted are for $k = 0$; only the Ψ_s component is shown.

tight binding model. Fig. 2(a) shows that for a value of $t_{sp} = 0.5$, the wave function calculated from with the fixed boundary condition differs significantly from that of the tight binding results for points close to the edge (near $y = 0$). The wavefunction with the natural boundary condition does not vanish at the boundary and has the expected exponential decay into the bulk. At large

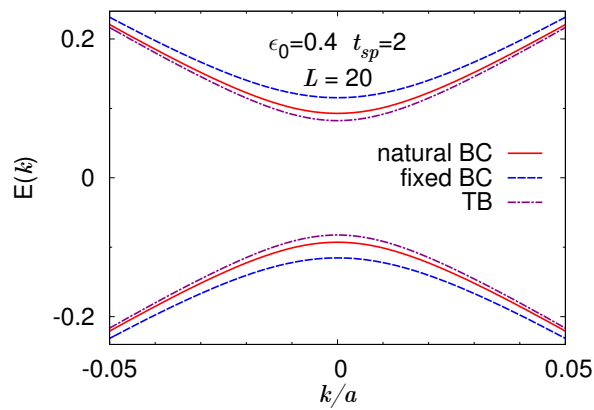
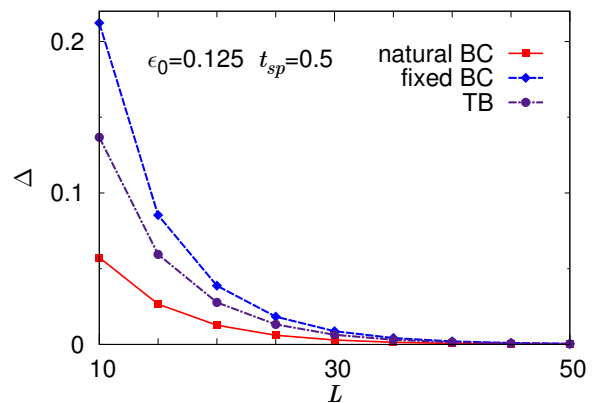


FIG. 3. Energy dispersion of edge states of a BHZ ribbon of width $L = 20$. For the parameter values shown, the continuum theory with the natural boundary condition (eqn. (15)) reproduces the tight binding result more accurately.

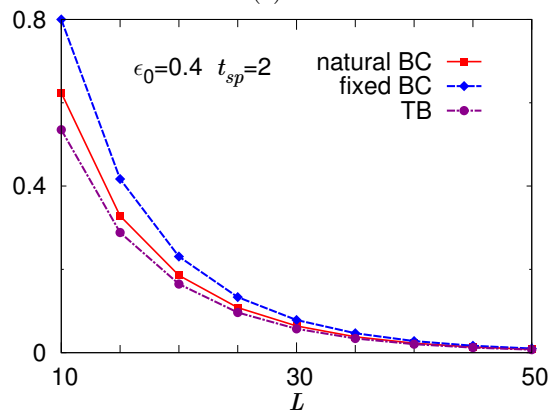
distances from the boundary the tight binding result for the wave function falls between the analytical results of the fixed and natural boundary conditions. This can be understood by noting that the fixed boundary condition kills the weight of the edge state near the boundary, and hence overestimates the weight of the wave function in the bulk. The effect is precisely the opposite with the natural boundary condition, where the weight in the bulk is underestimated compared to tight binding result. We now consider Fig. 2(b) which shows the comparison of the edge state wave function with $t_{sp} = 2$, but still with $\epsilon_0 < t_{sp}^2$. In this case we see that the wavefunction determined by the natural boundary condition not only closely reproduces the qualitative aspects of the tight binding solution, but is also in excellent quantitative agreement with it at large distance from the edge. Finally, in Fig. 2 we show the comparison of the wave functions in the regime of parameters with $\epsilon_0 > t_{sp}^2$. We see, again, that the analytical wave function obtained with the natural boundary condition more closely matches the results of tight binding calculation.

B. Ribbons

We now consider ribbons of finite width L . In this case, the edge states emanating from the edges at $y = 0$ and $y = L$, overlap and hybridize rendering the system gapped (see Fig. 3). A stronger test of the validity of the continuum formulation and the correctness of the boundary condition can be achieved by comparing the gap calculated using the analytical formulation with that obtained from the tight binding numerics. Fig. 4(a) shows the comparison of the calculated gaps as a function of the ribbon width L . In this regime of parameters the gap falls exponentially with the ribbon width as it is determined by the overlap matrix element of the two edge states emanating from the opposite edges. Again, we see that in



(a)



(b)

FIG. 4. Comparison of the energy gap obtained analytically by using the two different BCs with the corresponding result from the tight binding calculation.

this parameter regime, the tight binding gap lies between the fixed boundary condition result which is the largest, and the natural boundary condition value which is the smallest. This can be understood based on the result of the previous section. The weight of the edge state wave function in the bulk is overestimated by the use of the natural boundary condition and hence this gives rise to a larger gap owing to a larger overlap of the wavefunctions emanating from the opposite edges. For the same reason, the natural boundary condition underestimates the gap. For a larger value of t_{sp} , the natural boundary condition is in better quantitative agreement with the tight binding results. This owes, again to the fact that wave function is better estimated by the natural boundary condition.

Our final result pertains to the energy gap in ribbons with parameters in the regime $\epsilon_0 > t_{sp}^2$. Fig. 5 shows a plot of the gap as a function of the ribbon width in such a regime; we see that the gap is *non-monotonic*. Although the gap follows an exponential fall with increasing ribbon width, there are “magic widths” at which the gap is very small; indeed our analytical results with the natural boundary conditions does reproduce these features. The physics behind this phenomenon can be traced to

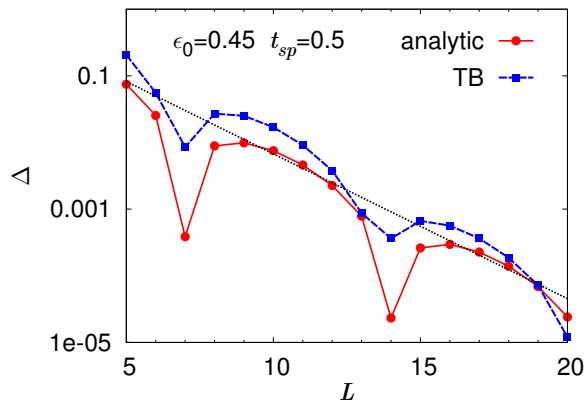


FIG. 5. Non-monotonic dependence of the energy gap with ribbon width L in the parameter regime $\epsilon_0 > t_{sp}^2$. The dashed line is a guide to the eye to show an overall exponential dependence on the ribbon width.

the oscillatory nature of the edge state wave function in this parameter regime; for some particular widths of the ribbon, there is a “near destructive interference” of the wave functions emanating from the opposite edges that renders their overlap matrix element small resulting in a smaller gap. To the best of our knowledge, this is the first report of such physics in the BHZ model. We believe this is generic, and in fact, can find possible use in the design nano-scale devices with topological insulators.

C. Discussion

As is evident from our results, a continuum field theory with a natural boundary condition provides an excellent description of systems with strong “component-mixing”. In the case of the BHZ model, this will occur when t_{sp} is large. Physically, in such cases a wave of “one flavour” can be reflected off a boundary as another flavor, and thus the wave functions do not have to vanish. This applies to the regime where the wave functions are

oscillatory in nature, the current brought about by one flavour can be reflected in another flavour channel. They may be contrasted with systems with a single component wave function such as in a simple “one component” tight binding model where the appropriate continuum boundary condition is that the vanishing of the wavefunction at the boundary. Topological insulators that are “deep” in their topological phase (such as a large ϵ_0 and t_{sp}) are strongly “multi-component” in nature. For such systems the natural boundary condition is more appropriate.

V. SUMMARY

In the paper, we have developed a continuum theory that is applicable to study four-band time reversal invariant systems. We formulate a variational energy functional and show that the Schrödinger equation in the bulk is the Euler-Lagrange equation of this functional. This formulation allows us to obtain the natural boundary condition of the system. We have compared our analytical results with full tight binding calculation for the BHZ model for the half-space and finite ribbons. We show that in the interesting topological regime, the natural boundary condition derived in this paper is more appropriate. We believe that our continuum formulation and boundary conditions will be useful in developing theory of devices and applications of topological insulators, and continuum theory modeling of experiments such as tunnelling from surface states. The non-monotonic dependence of the gap on the width of a BHZ ribbon is of particular interest; we believe such features are generic and can have numerous applications.

Acknowledgement

AM acknowledges support from CPDF programme at IISc, Bangalore. VBS thanks DST (Ramanujan grant) and DAE (SRC grant) for generous support.

* amedhi@physics.iisc.ernet.in

† shenoy@physics.iisc.ernet.in

¹ C. L. Kane and E. J. Mele, *Phys. Rev. Lett.* **95**, 146802 (2005).

² C. L. Kane and E. J. Mele, *Phys. Rev. Lett.* **95**, 226801 (2005).

³ B. A. Bernevig, T. L. Hughes, and S.-C. Zhang, *Science* **314**, 1757 (2006).

⁴ M. Z. Hasan and C. L. Kane, *Rev. Mod. Phys.* **82**, 3045 (2010).

⁵ X.-L. Qi and S.-C. Zhang, *Rev. Mod. Phys.* **83**, 1057 (2011).

⁶ J. E. Moore, *Nature* **464**, 194 (2010).

⁷ M. König, S. Wiedmann, C. Brune, A. Roth, H. Buhmann, L. W. Molenkamp, X.-L. Qi, and S.-C. Zhang, *Science* **318**, 766 (2007).

⁸ M. König, H. Buhmann, L. W. Molenkamp, T. Hughes, C.-X. Liu, X.-L. Qi, and S.-C. Zhang, *J. Phys. Soc. Jpn.* **77**, 031007 (2008).

⁹ B. Zhou, H.-Z. Lu, R.-L. Chu, S.-Q. Shen, and Q. Niu, *Phys. Rev. Lett.* **101**, 246807 (2008).

¹⁰ K.-I. Imura, A. Yamakage, S. Mao, A. Hotta, and Y. Kuramoto, *Phys. Rev. B* **82**, 085118 (2010).

¹¹ S. Mao, Y. Kuramoto, K.-I. Imura, and A. Yamakage, *J. Phys. Soc. Jpn.* **79**, 124709 (2010).

¹² S. Mao, A. Yamakage, and Y. Kuramoto, *Phys. Rev. B* **84**, 115413 (2011).

- ¹³ M. Hohenadler, T. C. Lang, and F. F. Assaad, *Phys. Rev. Lett.* **106**, 100403 (2011).
- ¹⁴ C. Wu, B. A. Bernevig, and S.-C. Zhang, *Phys. Rev. Lett.* **96**, 106401 (2006).
- ¹⁵ C. Xu and J. E. Moore, *Phys. Rev. B* **73**, 045322 (2006).
- ¹⁶ L. Brey and H. A. Fertig, *Phys. Rev. B* **73**, 195408 (2006).
- ¹⁷ A. R. Akhmerov and C. W. J. Beenakker, *Phys. Rev. B* **77**, 085423 (2008).
- ¹⁸ A. H. Castro Neto, F. Guinea, N. M. R. Peres, K. S. Novoselov, and A. K. Geim, *Rev. Mod. Phys.* **81**, 109 (2009).
- ¹⁹ S. Bhowmick and V. B. Shenoy, *Phys. Rev. B* **82**, 155448 (2010).
- ²⁰ J. A. M. van Ostaay, A. R. Akhmerov, C. W. J. Beenakker, and M. Wimmer, *Phys. Rev. B* **84**, 195434 (2011).
- ²¹ I. M. Gelfand and S. V. Fomin, *Calculus of variations* (Prentice Hall, Englewood Cliffs, N. J., 1965).
- ²² A. Medhi, V. B. Shenoy, and H. R. Krishnamurthy, *arXiv:1112.4308v1* (2011).
- ²³ R. Takahashi and S. Murakami, *Phys. Rev. B* **81**, 161302 (2010).
- ²⁴ P. Ghaemi, R. S. K. Mong, and J. E. Moore, *Phys. Rev. Lett.* **105**, 166603 (2010).
- ²⁵ S. Murakami, N. Nagaosa, and S.-C. Zhang, *Science* **301**, 1348 (2003).
- ²⁶ S. Murakami, N. Nagaosa, and S.-C. Zhang, *Phys. Rev. B* **69**, 235206 (2004).
- ²⁷ K. Gottfried and T.-M. Yan, *Quantum Mechanics: Fundamentals* (Springer, 2003).
- ²⁸ J. E. Moore and L. Balents, *Phys. Rev. B* **75**, 121306 (2007).
- ²⁹ R. Roy, *Phys. Rev. B* **79**, 195321 (2009).
- ³⁰ R. Roy, *Phys. Rev. B* **79**, 195322 (2009).